Supporting Information

El Helou et al. 10.1073/pnas.1221381110

SI Materials and Methods

Protocol. Sleep deprivation (SD) was performed for 6 h from Zeitgeber time 0 (ZT0; the onset of the light period) to ZT6 by gentle handling (1). Sleep-deprived mice, except mice used for EEG recording, were killed at ZT6 together with undisturbed (nonsleep deprived) control mice. For around the clock experiments (Fig. 4 *A* and *C*), mice were killed at 6-h intervals. Upon sacrifice, brains were immediately extracted and frozen on dry ice or liquid nitrogen.

Reverse Transcription and Quantitative PCR. RNA extraction and reverse transcription were performed as detailed before (2–4). Briefly, RNA was extracted from the forebrain using the RNeasy Lipid Tissue Midi kit and was Dnase-treated (Qiagen). RNA amount was verified with a NanoDrop ND-1000 or ND-2000 spectrophotometer (Thermo Scientific), and the quality of RNA samples was verified on Agilent 2100 bioanalyzer chips (Agilent Technologies) or by using agarose gel electrophoresis. Then, 0.5–3 μg of RNA was used for reverse transcription using random hexamers and SuperScript II or III reverse transcriptase (Invitrogen), according to standard procedures. Quantitative PCR (qPCR) was performed using an ABI PRISM 7900 detection system (Applied Biosystems) or a Viia 7 real-time cycler (Life Technologies). Individual mouse cDNA was diluted and used in a 10-μL reaction with TaqMan Master Mix reagent (Applied Biosystems/Life Technologies) under standard cycling conditions: 95 °C for 10 min, followed by 40 cycles of 95 °C for 15 s and 60 °C for 1 min. Assays were designed at an exon–exon junction using Primer Express (Applied Biosystems), and the absence of DNA polymorphism in the target sequences was confirmed by BLAST searches against available web database (except D2 mice polymorphism rs29588067 present in probe set targeting *Nlg1* with insert A that could not be avoided). Primers were purchased from Invitrogen, Life Technologies, Operon, or Microsynth and probes were purchased from Eurogentec or Operon. Sequences are provided in Table S1. TaqMan Gene Expression Assay #Mm04230607_s1 was used for mouse brain derived neurotrophic factor (*mBdnf*), Mm00433790_m1 for N-methyl-D-aspartate receptors (NMDAR) subunit 1 (*Nr1*), Mm00433802_m1 for NMDAR subunit 2a (*Nr2a*), Mm00433820_m1 for NMDAR subunit 2b (*Nr2b*), Mm01341723_m1 for NMDAR subunit 3a (*Nr3a*), and Mm00504568_m1 for NMDAR subunit 3b (*Nr3b*). Each PCR was done in triplicate. The most stable endogenous controls were selected among *Actin*, TATA box binding protein (*Tbp*), Beta-glucuronidase (*GusB*), and *Ribosomal protein S9* (Rps9) using geNorm v3.5 (5) or Expression Suite v1.0 (Life Technologies), and two (Fig. 1*B*) or three (Figs. 1*C*, 3*F*, and 4*A*) controls were used for normalization. Relative quantification was calculated using the modified ΔΔCt method from qBase v1.3.5 (6) or Expression Suite v1.0.

Protein Extraction and Western Blotting. At the end of SD, brains from C57BL/6J (B6) and AKR/J (AK) mice were rapidly removed, dissected, and frozen in liquid nitrogen. Dissection involved removal of cerebellum and olfactory bulbs and separation of the anterior and posterior part of the brain relative to the bregma. Total (Tot) and synaptoneurosomal (SN) protein extractions were done similarly as previously described (7). Briefly, brains were washed with cold PBS and homogenized in SN lysis buffer [10 mM Hepes, pH 7.4, 1 mM EDTA, 2 mM EGTA, 0.5 mM DTT, phosphatase, and protease inhibitors mixture 1:100 (Sigma Aldrich)] using a rotor stator homogenizer (Fisher Scientific). A volume was sonicated (Q Sonica) and centrifuged for 2 min at 16,200 × *g*, and the supernatant represented the total protein fraction. The remaining fraction of the homogenate was mixed with lysis buffer, centrifuged for 2 min at 2,000 × *g*, and the supernatant was filtered using a 10-μm pore nylon mesh filter (Small Parts Inc.) and then a 5-μm pore centrifugal filter (Ultrafree-CL, Millipore) and further centrifuged at 5,000 × *g* for 15 min. The pellet was resuspended in boiling lysis buffer and represented the SN protein fraction. To further purify protein extracts, a 1:1 (Tot) or 1:1.5 (SN) ratio of protein:buffer was centrifuged at 16,200 × *g* for 2 min (Tot) or 2,000 × *g* for 2 min (SN). Protein concentration was determined using the Lowry Assay and a Nanodrop ND-2000 (Thermo Scientific). Forty micrograms (Tot) or 25 μg (SN) of proteins were loaded on 7.5% precast SDS/PAGE gels (Bio-Rad Laboratories) and transferred onto nitrocellulose membranes.

Blots were blocked for 30 min in Phosphate buffered saline with Tween 20 containing 5% (wt/vol) nonfat dry milk. Antibodies used were mouse anti-Neuroligin 1 (1:1,000; Synaptic Systems; #129 111), mouse anti-Actin (1:10,000; Sigma Aldrich; #A5441), and HRP-conjugated donkey anti-mouse (1:2,500; Santa Cruz Biotechnology; #sc-2318). Membranes were revealed using an Immun-Star Chemiluminescent kit (Bio-Rad), signal quantification was done using QuantityOne (Bio-Rad), and Neuroligin-1 (NLG1) level was normalized relative to Actin.

Electroencephalography/Electromyography Electrode Implantation Surgery. We used knockout (KO) mice for the *Nlg1* gene (mouse line B6;129-*Nlgn1*^{tm1Bros}/J) and their WT littermates, which are normal and fertile. Electrode implantation for electroencephalography (EEG) and electromyography (EMG) recording was performed as detailed previously (2, 3). Briefly, when mice reached 9–10 wk, surgery was performed under deep Ketamine/Xylazine anesthesia (120/10 mg/kg, i.p. injection). Two gold-plated screws (diameter: 1.1 mm) served as EEG electrodes and were screwed through the skull over the right cerebral hemisphere (anterior: 1.7 mm lateral to midline, 1.5 mm anterior to bregma; posterior: 1.7 mm lateral to midline, 1.0 mm anterior to lambda). An additional screw placed on the right hemisphere (6 mm lateral to midline, 3 mm posterior to bregma) served as a reference. Three other screws were implanted over the left hemisphere as anchors. Two gold wires served as EMG electrodes and were inserted between neck muscles. The EEG and EMG electrodes were soldered to a connector and, together with the anchor screws, cemented to the skull. Four days after surgeries, mice were connected to a swivel contact, and animals were allowed a week of habituation before recording.

EEG Recording and Analyses. EEG/EMG was recorded continuously for 48 h starting at light onset. Signals were amplified (Lamont amplifiers), sampled at 256 Hz, and filtered using the software Stellate Harmonie (Natus). Behavioral states [wakefulness, nonrapid eye movement (NREM) sleep, and rapid eye movement (REM) sleep] were visually assigned to 4-s epochs, as previously described (8), and artifacts were simultaneously identified. The duration of each state was averaged for the full 24 h, the first 12 h (light period), the second 12 h (dark period), and per hour. Spectral analysis was performed on the bipolar EEG signal of artifact-free epochs using fast Fourier transform to calculate the EEG power density between 0.5 and 20 Hz (0.25 Hz resolution) during wakefulness, NREM, and REM sleep for the first 24 h of the recording. Delta power (1–4 Hz EEG activity) during NREM sleep was also separately computed and averaged for 12 intervals

during the light period, for which an equal number of epochs contributed, for 8 intervals during the 6 h immediately following SD and for 6 intervals during the dark periods.

ChIP. Chromatin extraction and immunoprecipitation was performed using the Magna ChIP G commercial kit (Millipore) according to the manufacturer's instructions (9). Cortices were chopped in small pieces and incubated for 10 min in 1% formaldehyde followed by a 5-min glycine quenching. After washes and cellular and nuclear lysis, chromatin breakdown to 300–1,000 bp was performed with a Bioruptor UCD-200TO (Diagenode). A preclear step was performed (1 h at 4 °C with 40 μL of magnetic beads) before overnight incubation of chromatin and beads with antibodies. Anti-Aryl hydrocarbon receptor nuclear translocator-like (Arntl) transcript variant 1 (BMAL1) antibody was purchased from Abcam (#ab3350) and anti-CLOCK from Abcam (#ab461) or Santa Cruz Biotechnology (#sc-6927). All samples were also identically submitted to a no-antibody condition (mock condition) used to take into account nonspecific binding. DNA purification was performed using the silica columns provided with the kit (Magna ChIP G, Millipore). For qPCR, the amplicon targeted a canonical E-box (CACGTG) located at position −653:−658 of the *Nlg1* gene (Table S1) and was designed with Primer Express v2.0 (Applied Biosystems). Purified immunoprecipitated DNA was slightly diluted (4/5) and mixed with 0.9 mM of each primer, 0.25 mM of probe, and Taqman MasterMix reagent (Applied Biosystems) or FastStart Universal Probe Master (Roche Diagnostic), and standard cycling conditions were used (see above).

Statistical Analyses. The effect of SD on the expression of *Nlg1* transcript variants was assessed using two-way analyses of variance (ANOVAs) with the factors "group" (B6 vs. AK or Sham vs. adrenalectomy) and "condition" (control vs. SD). The effect of SD on Tot and SN levels of NLG1 in the two brain regions was compared between control and SD mice using paired *t* tests. The *t*-tests were also used to compare, between genotypes, the duration of vigilance states and of wake bouts per 24 or 12 h, spectral activity per 0.25 Hz, NREM sleep during SD, NREM sleep loss with SD, and the latency to sleep onset. Hourly duration of vigilance states, time course of delta power, and time course of accumulated differences in NREM sleep time were compared using two-way repeated-measure ANOVAs with the factors "genotype" (WT vs. KO) and "hour" or "interval." The effect of genotype and SD on gene expression was assessed using two-way ANOVAS with the factors "genotype" (WT vs. KO) and "condition" (control vs. SD). To assess the effect of time of day on the expression of *Nlg1* transcript variants, we used two-way ANOVAs with the factors "strain" (B6 vs. AK) and "time" (ZT0, -6, -12, and -18). For the ChIP experiment, one-way ANOVAs with the factor "time" (ZT0, -6, -12, -18) were performed, and the effect of SD on clock genes was analyzed using single sample *t*-tests. Significant effects were decomposed, when appropriate, using planned comparisons, and significance levels for repeated measures were corrected using the Huynh–Feldt correction. Statistical analyses were performed using Statistica (StatSoft Inc.). Significance threshold was set to 0.05, and data are reported as mean ± SEM. The number of animals used for each experiment is reported in figure legends.

Assessment of Social Interaction Behavior. A three-chamber paradigm was used to assess social interaction behavior in *Nlg1* KO mice (10). Briefly, animals were handled and habituated to the experimental room and set up for 1 wk before testing. Mice behavior was observed, timed, and video-recorded over two 10-min sessions. For the first session, the test mouse was exposed to an empty cage and a cage containing a stranger mouse of the same age and sex. Total interaction time (e.g., nose touching, sniffing, climbing) and number of interactions with both the empty cage and the stranger mouse were measured during the session. For the second session, the empty cage was replaced by a new (nonfamiliar) stranger mouse, and total interaction time and number of interactions with both the familiar mouse (from session 1) and the new stranger mouse were measured. The object mice (confined to cages) were randomly assigned to each chamber and had been previously habituated to cage confinement. Preference for social interaction and social novelty was assessed using two-way ANOVAs with the factors genotype (WT vs. KO) and "stranger" (empty cage vs. stranger 1 or stranger 1 vs. stranger 2).

Neurological Severity Test. Neurological function was assessed in WT and *Nlg1* KO mice using a standardized 10-point Neurological Severity Score (NSS) as previously described (11, 12). This abbreviated version of the original 25-point scale (13) includes 10 individual parameters that are easy to assess and relatively independent of the investigator's subjective evaluation. The 10 parameters are representative of overall motor function, alertness, and physiological behavior, where no point was given for a successfully executed task and one point was given for failing. A maximum NSS score of 10 points indicates severe neurological impairments with failure at all tasks and a minimal score of zero refers to a normally behaving mouse. To control for possible time-of-day effect, the NSS test was administered at ZT0 (beginning of the rest period) and ZT11 (end of the rest period, beginning of the active period). However, a genotype-by-time ANOVA revealed no significant effect of time of day, and data were therefore presented as a mean of the two times and compared between genotypes using a *t*-test.

Optical Imaging of the Brain Hemodynamic Response. The brain hemodynamic response to somatosensory stimulation was assessed in *Nlg1* KO mice using multispectral optical imaging as previously described (14). Briefly, under deep anesthesia (Ketamine/Xylazine, 120/10 mg/kg), the skull was exposed and mice were positioned on a stereotaxic frame. Two electrodes were placed on each side of the left forepaw for stimulation using an electrical stimulator (A-M Systems; #2200). The threshold for muscle response was determined using a 0.3-ms pulse and increasing current intensity. The mean threshold was 0.86 ± 0.027 mA and did not differ significantly between genotypes (WT: 0.95 ± 0.06; KO: 0.81 ± 0.05; $P = 0.08$). For imaging, twofold-threshold intensity was used for electrical stimulation (3 Hz, 300 μs, between 1 and 2.6 mA), and stimulations were repeated every 20 s with a 1- to 3-s random jitter to avoid systemic synchronization. Mineral oil was added to the skull to prevent drying and maintain camera focus. Functional images (typical size 450 × 400 pixels) were recorded under a multiple wavelength flashing illumination (525, 590, and 637 nm) produced by light-emitting diodes (LED) (Optek Technologies) at a sampling rate of 5 Hz per wavelength using a 12-bit CCD camera (CS3960DCL; Toshiba Teli). Reflectance signals from the LED collected with the camera were converted into changes in absorption for the three wavelengths, followed by extraction of relative changes in oxyhemoglobin (HbO) and deoxyhemoglobin (HbR) using a modified Beer–Lambert law (14, 15).

Spatial *t*-statistic HbO and HbR response maps were constructed from the mean and SEM of the early and filtered response to all stimulations. This was calculated for each pixel by taking the mean between 1 and 3 s after stimulation, expressed relative to the median of 2 s before stimulation on temporally high-pass-filtered (0.03-Hz cutoff) and spatially low-pass-filtered data (Gaussian, 0.5 pixel SD). Animals that did not respond on these maps were removed from further analysis ($n = 2$). For each mouse, a region of interest (ROI; fixed size of 75 × 75 pixels) was selected to cover the right somatosensory cortex (contralateral).

Then, after standard bandpass filtering of the raw data between 0.01 and 0.67 Hz, time courses of the relative changes were built for HbO and HbR for the selected ROI as a function of the median of 3 s before stimulation. Only responses with an observable peak in HbO combined with a decrease in HbR between 1 and 5 s poststimulation were kept to construct the mean time course of one animal. The percentage of response was calculated as the number of responses divided by the total number of stimulations multiplied by 100. One mouse was excluded because it did not show either a 50% response rate or 10 observable responses. Percentage of response was compared between genotypes using a *t*-test, and time courses of HbO and HbR were compared using genotype-by-time ANOVAs with degrees of freedom adjusted for nonsphericity using the Greenhouse–Geisser method.

1. Franken P, Dijk DJ, Tobler I, Borbély AA (1991) Sleep deprivation in rats: Effects on EEG power spectra, vigilance states, and cortical temperature. *Am J Physiol* 261(1 Pt 2):R198–R208.
2. Mongrain V, et al. (2010) Separating the contribution of glucocorticoids and wakefulness to the molecular and electrophysiological correlates of sleep homeostasis. *Sleep* 33(9):1147–1157.
3. Curie T, et al. (2013) Homeostatic and circadian contribution to EEG and molecular state variables of sleep regulation. *Sleep* 36(3):311–323.
4. Franken P, Thomason R, Heller HC, O'Hara BF (2007) A non-circadian role for clock-genes in sleep homeostasis: A strain comparison. *BMC Neurosci* 8:87.
5. Vandesompele J, et al. (2002) Accurate normalization of real-time quantitative RT-PCR data by geometric averaging of multiple internal control genes. *Genome Biol* 3(7):RESEARCH0034.
6. Hellemans J, Mortier G, De Paepe A, Speleman F, Vandesompele J (2007) qBase relative quantification framework and software for management and automated analysis of real-time quantitative PCR data. *Genome Biol* 8(2):R19.
7. Seibt J, et al. (2012) Protein synthesis during sleep consolidates cortical plasticity in vivo. *Curr Biol* 22(8):676–682.
8. Franken P, Malafosse A, Tafti M (1999) Genetic determinants of sleep regulation in inbred mice. *Sleep* 22(2):155–169.
9. Mongrain V, La Spada F, Curie T, Franken P (2011) Sleep loss reduces the DNA-binding of BMAL1, CLOCK, and NPAS2 to specific clock genes in the mouse cerebral cortex. *PLoS ONE* 6(10):e26622.
10. Kaidanovich-Beilin O, Lipina T, Vukobradovic I, Roder J, Woodgett JR (2011) Assessment of social interaction behaviors. *J Vis Exp* Feb 48:2473.
11. Flierl MA, et al. (2009) Mouse closed head injury model induced by a weight-drop device. *Nat Protoc* 4(9):1328–1337.
12. Stahel PF, et al. (2000) Experimental closed head injury: Analysis of neurological outcome, blood-brain barrier dysfunction, intracranial neutrophil infiltration, and neuronal cell death in mice deficient in genes for pro-inflammatory cytokines. *J Cereb Blood Flow Metab* 20(2):369–380.
13. Chen Y, Constantini S, Trembovler V, Weinstock M, Shohami E (1996) An experimental model of closed head injury in mice: Pathophysiology, histopathology, and cognitive deficits. *J Neurotrauma* 13(10):557–568.
14. Dubeau S, Ferland G, Gaudreau P, Beaumont E, Lesage F (2011) Cerebrovascular hemodynamic correlates of aging in the Lou/c rat: A model of healthy aging. *Neuroimage* 56(4):1892–1901.
15. Dunn AK, et al. (2003) Simultaneous imaging of total cerebral hemoglobin concentration, oxygenation, and blood flow during functional activation. *Opt Lett* 28(1):28–30.

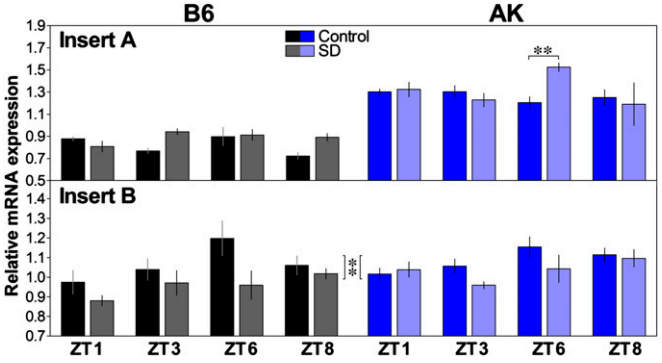

Fig. S1. Relative expression of *Nlg1* with insert A and with insert B in the forebrain measured by qPCR in C57BL/6J (B6) and AKR/J (AK) mice at ZT1 (1 h after light onset), at ZT3 and ZT6 in control condition or after 1, 3, and 6 h of SD, respectively, and at ZT8 in control condition or after a 6-h SD followed by 2 h of recovery sleep ($n = 4$/group except $n = 3$ for B6 mice after recovery and for AK mice with 3 h of SD for *Nlg1* with B). A "strain-by-condition-by-time" interaction showed that *Nlg1* with A was increased in AK mice only after 6 h of SD ($F_{3,47} = 3.8$, $P < 0.05$; $^{**}P < 0.01$ between indicated values). For *Nlg1* with B, a significant effect of condition ($F_{1,46} = 9.5$, $^{**}P < 0.01$) showed that SD decreased its expression, and a significant effect of time ($F_{3,46} = 4.1$, $P < 0.05$) showed that expression was higher at ZT6 than at ZT1 and ZT3 and at ZT8 compared with ZT1.

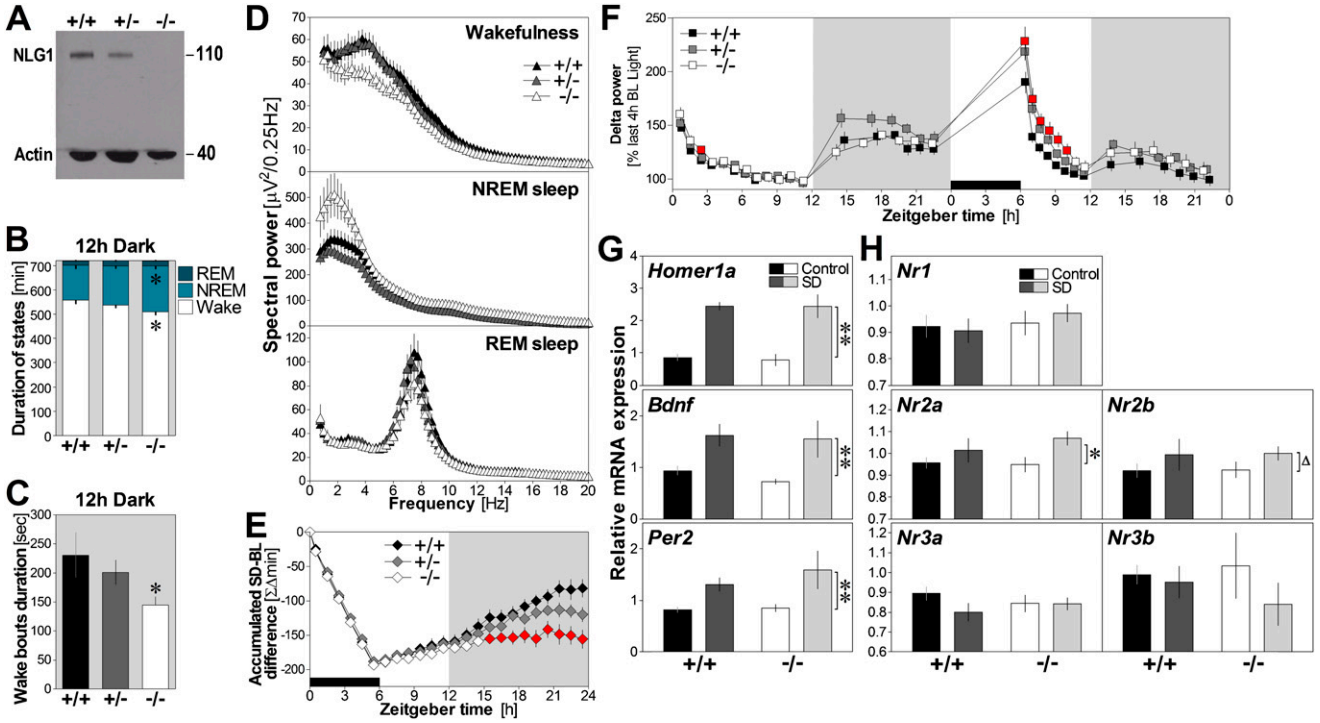

Fig. S2. (*A*) Blot showing forebrain NLG1 level in a WT (+/+), a heterozygous (+/–), and a *Nlg1* KO (–/–) mouse, and the endogenous control Actin. (*B*) Vigilance states duration in WT ($n = 10$), heterozygous ($n = 14$), and *Nlg1* KO ($n = 12$) mice for the 12-h dark period. KO mice spend less time in wakefulness and more in NREM sleep than WT ($F_{2,33} \geq 3.4$, $P < 0.05$). Heterozygous mice did not significantly differ from WT or KO. (*C*) Mean duration of wake bouts in WT, heterozygous, and KO mice for the 12-h dark period. Duration of wake bouts tend to differ with genotype [$F_{2,33} = 2.9$, $P < 0.07$; *t*-test between WT and KO, $^{*}P < 0.05$ (see main text)]. (*D*) Spectral power for the three behavioral states in WT, heterozygous, and KO mice. (*E*) Time course of accumulated differences in NREM sleep between the 6-h SD followed by 18 h of recovery and baseline (BL) conditions in WT, heterozygous and KO mice. Significant genotype-by-time interaction was found ($F_{46,759} = 5.4$, $P < 0.001$). Heterozygous mice differed from WT for the last hour only and from KO for the last 7 h. Differences between KO and WT are indicated by red symbols ($P < 0.05$; same in *F*). (*F*) Forty-eight-hour time course of relative delta power (% of the last four intervals of the BL light period) in WT, heterozygous, and KO mice. Genotype-by-time interaction was found for the full 48-h recording ($F_{62,961} = 2.2$, $P < 0.05$). Gray backgrounds indicate dark periods and black rectangles the 6-h SD. (*G*) Relative expression of Homer homolog 1 a (*Homer1a*), *Bdnf*, and Period 2 (*Per2*) in the forebrain of WT and *Nlg1* KO mice measured by qPCR at ZT6 in control condition or after a 6-h SD ($n = 6$/group). Condition effects revealed that SD significantly increased the expression of all three genes in both genotypes ($F_{1,20} > 9.6$, $^{**}P \leq 0.005$). (*H*) Relative expression of *N*-methyl-D-aspartate receptor subunits in the forebrain of WT and *Nlg1* KO mice measured by qPCR at ZT6 in control condition or after a 6-h SD ($n = 6$/group). Condition effect showed that SD increased the expression of *Nr2a* in both genotypes ($F_{1,20} = 5.8$, $^{*}P < 0.05$). A similar trend was observed for *Nr2b* ($F_{1,20} = 2.7$, $^{\Delta}P = 0.1$).

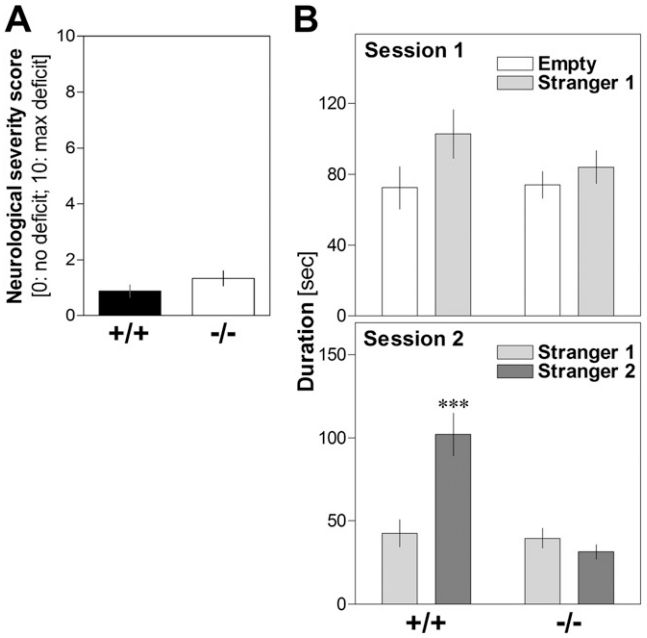

Fig. S3. (*A*) NSS in WT and *Nlg1* KO mice (mean of two tests performed at ZT0 and ZT11, $n = 12$ per genotype). NSS did not differ between genotypes ($t = -1.3$, $P > 0.2$). (*B*) Social behavior in *Nlg1* KO mice and WT littermates. Two-way repeated measure ANOVA with factors genotype (+/+ vs. –/–) and stranger (empty vs. stranger 1) showed a stranger effect for session 1 ($F_{1,13} = 5.3$, $P < 0.05$), with mice spending more time interacting with the stranger mouse compared with the empty cage. For session 2, a significant genotype-by-stranger (stranger 1 vs. stranger 2) interaction was observed showing that only WT spend more time interacting with the new stranger mouse 2 compared with the familiar stranger mouse 1 ($F_{1,13} = 72.3$, $P < 0.001$). ***$P < 0.001$ compared with stranger 1 for WT.

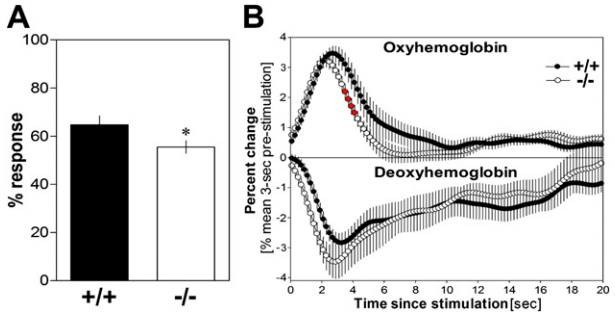

Fig. S4. (*A*) Percentage of response of brain hemodynamic parameters to forepaw stimulation in WT ($n = 11$) and *Nlg1* KO ($n = 16$) mice. Compared with WT, KO mice showed a lower percentage of response to stimulation ($t = 2.1$, $P < 0.05$). (*B*) Oxy- and deoxyhemoglobin response of the cerebral cortex following forepaw stimulation for WT and *Nlg1* KO mice. Analysis of the first 5 s after stimulation revealed a significant genotype-by-time interaction for oxyhemoglobin ($F_{24,600} = 4.0$, $P < 0.05$) with KO mice showing lower levels at 4 s poststimulation (red symbols: $P \leq 0.05$ compared with WT). For deoxyhemoglobin, only a significant time effect was observed ($F_{24,600} = 33.1$, $P < 0.001$; group-by-time interaction: $F_{24,600} = 0.7$, $P = 0.8$).

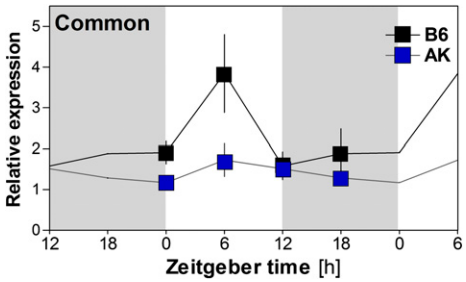

Fig. S5. Relative mRNA expression of the common *Nlg1* transcript measured at ZT0 (light onset), ZT6, ZT12 (light offset), and ZT18 by qPCR in the forebrain of C57BL/6J (B6) and AKR/J (AK) mice ($n = 5$–8/group). Strain-by-time ANOVA revealed that the expression is affected by time ($F_{3,47} = 3.1$, $P = 0.03$) with highest level at ZT6. A significant effect of strain was also observed ($F_{1,49} = 4.4$, $P < 0.05$) with B6 mice showing a higher expression.

Table S1. Sequences of primers and probes used for qPCR

Gene symbol	Direction	Sequence 5′ to 3′	Accession no.
mNlg1A	Foward	ACGGTGCTGAAGATGAAG	NM_001163387
	Reverse	CAGTACCTTCCATGTAAGAG	
	Probe	TCCCAAACCAGTGATGGTGTACATCCA	
mNlg1NA	Foward	GGATGTGGTTTCATCATAC	NM_001163387
	Reverse	TGTCCCGAATATCATCTTC	
	Probe	TCCAAGACCAGAGTGAAGACTGTC	
mNlg1B	Foward	GGTAACCGTTGGAGCAATTCA	NM_001163387
	Reverse	CCAGCTGGAAAGGGCTGTT	
	Probe	CCAAAGGACTTTTTCAACGAGCAATAGCTCA	
mNlg1NB	Foward	CACTGTGTTTGGATCAGG	NM_001163387
	Reverse	AAAAGTCCTTCAGAATAATGGG	
	Probe	GGTTCATGTGTCAACCTGCTGACT	
mNlg1C	Foward	TCCTTGCAATTTCTCCAAGA	NM_001163387
	Reverse	TTGGGTTTGGTATGGATGAA	
	Probe	TGGTGACCCAAATCAACCAGTTCC	
mNlg1 E-box	Foward	TGGGAAAATATCTTTGGCCTATAAAA	NT_162143.3
	Reverse	GCACGGAAAGTGCCATGAA	
	Probe	AGGTGGCAATTTCTTTCTCTTCTACACGTGG	
mHomer1a	Foward	GCATTGCCATTTCCACATAGG	NM_011982
	Reverse	ATGAACTTCCATATTTATCCACCTTACTT	
	Probe	ACACATTCAATTCAGCAATCATGA	
mPer2	Foward	ATGCTCGCCATCCACAAGA	NM_011066
	Reverse	GCGGAATCGAATGGGAGAAT	
	Probe	ATCCTACAGG CCGGTGGACAGCC	
mRps9	Foward	GACCAGGAGCTAAAGTTGATTGGA	NM_029767
	Reverse	TCTTGGCCAG GGTAAACTTGA	
	Probe	AAACCTCACGTTTGTTCCGGAGTCCATACT	
mActin	Foward	CTAAGGCCAACCGTGAAAAGAT	NM_007393
	Reverse	CACAGCCTGGATGGCTACGT	
	Probe	TTGAGACCTTCAACACCCCAGCCATG	
mGusB	Foward	ACGGGATTGTGGTCATCGA	NM_010368
	Reverse	TGACTCGTTGCCAAAACTCTGA	
	Probe	AGTGTCCCGGTGTGGGCATTGTG	
mTbp	Foward	TTGACCTAAAGACCATTGCACTTC	NM_013684
	Reverse	TTCTCATGATGACTGCAGCAAA	
	Probe	TGCAAGAAATGCTGAATATAATCCCAAGCG	

mNlg1, mNeuroligin 1; *mNlg1A*, mNeuroligin 1 with insert A; *mNlg1Na*, mNeuroligin 1 without insert A; *mNlg1B*, mNeuroligin 1 with insert B; *mNlg1NB*, mNeuroligin 1 without insert B; *mNlg1C*, mNeuroligin 1 common probe.